

# Chapter 6

## Protonated Ammonia Clusters

### 6.1 Introduction

Hydrogen bonding governs a number of diverse and important chemical interactions, ranging from the solvent properties of water and other liquids to the structure of proteins and nucleic acids [198]. Hydrogen bonds control transport mechanisms such as water channels [199] and proton wires or proton pumps [200–203]. In recent years, several studies on ammonia concentrated on transport phenomena equivalent to those in which water is involved. Khademi et al. [204], for example, resolved a crystallographic structure of a bacterial ammonia transport channel, AmtB. At the two ends of the pore, broader vestibules contain  $\text{NH}_3$  in equilibrium with  $\text{NH}_4^+$  in water. AmtB has at its center a narrow hydrophobic pore element, which allows the passage of  $\text{NH}_3$  but not the monovalent ion  $\text{NH}_4^+$  [205]. Meuwly et al. studied the proton transfer along ammonia wires [206, 207]. Bach et al. [208] studied the proton donor-acceptor system 7-hydroxyquinoline $\cdot(\text{NH}_3)_n$  ( $n \leq 10$ ). For this system the results suggest that proton transfer, which may occur along an ammonia wire, triggers the isomerization reaction  $\text{enol7-HQ}\cdot(\text{NH}_3)_n \rightarrow \text{keto7-HQ}\cdot(\text{NH}_3)_n$  for  $n \leq 10$ .

All these dynamical processes are governed by the interaction potential between the atomic and molecular constituents. Nevertheless, an accurate microscopical description of the hydrogen bond interaction is difficult because of the complexity of treating the thermal and quantum fluctuations of many atoms in conjunction with a highly accurate description of both the covalent and dispersive interactions [209]. Hydrogen bonds are very sensitive to perturbation, due to an intimate interdependence between heavy atom separation, H-atom exchange barrier and position of the light H-atom leading to unusually high proton polarizability in strong H-bonds. Therefore it can prove advantageous to study hydrogen bonds in model systems in the gas phase, in the absence of any perturbations from surrounding solvent or host molecules. Standard experimental techniques to study strong hydrogen bonds, including NMR, as well as

X-ray and neutron diffraction, are currently limited to condensed phase probes. Many gas phase experiments are hindered by low number densities while IR-PD exhibits the required sensitivity and selectivity to perform such studies. Moreover, hydrogen bonds are particularly appealing from the perspective of cluster spectroscopy, which can probe how the properties of a collection of molecules held together by hydrogen bonds evolve with size [210].

Dawson and Tickner [211] first identified the cluster ions  $\text{NH}_4^+(\text{NH}_3)_n$ ,  $n \leq 4$ , in the gas phase mass spectrometrically, which exist as the major ionic species in the negative glow of DC discharges in ammonia. Gas-phase studies which followed centered, for the most part, on the thermodynamics and kinetics of clustering reactions at relatively high pressures [212,213]. Kebarle and coworkers [212,214] showed that in the larger clusters there was a discontinuity in the formation enthalpy for the  $n = 4 \rightarrow n = 5$  clustering step, consistent with the idea that there were four solvent molecules (ammonia) involved in the first solvation shell of the ammonium ion. This picture was based on the results of early spectroscopic studies on the ammonium ion in the condensed phase by direct IR absorption measurements of either crystals of ammonium salts or ammonium salts dissolved in solution [215,216]. These measurements revealed spectral features that were assigned to vibrational modes of the perturbed  $\text{NH}_4^+$  ion ( $T_d$  symmetry).

Schwarz [217] measured the gas phase spectra of the ammoniated ammonium ion for  $n=1-4$  in the 2–5  $\mu\text{m}$  region by direct absorption measurements in a pulsed radiolysis of a gas cell containing ammonia in a helium carrier. These measurements made use of the known equilibrium constants for the clustering reactions to deconvolute the absorption signal obtained at various pressures into those of individual ammoniated ammonium ions. With these pioneering measurements, Schwarz was able to observe the vibrational bands  $\nu_3$  and  $2\nu_4$  of the ammonium ion core for the  $n=4$  ion cluster, and showed also that the  $n=4$  cluster ion is tetrahedral, while the  $n=3$  one was consistent with a  $C_{3v}$  symmetry (see Figure 6.1). In 1991 Lee and coworkers [218] applied IR-PD spectroscopy to study the gas phase vibrational spectra of mass selected ammoniated ammonium ions,  $\text{NH}_4^+(\text{NH}_3)_n$  for  $n = 1-10$ , in the region from 2600 to 4000  $\text{cm}^{-1}$  by IR-PD. They used a pulsed, infrared laser tunable in the 2600–4000  $\text{cm}^{-1}$  region, coupled with a CW  $\text{CO}_2$  laser. The first pulse selectively excited the clusters and then the  $\text{CO}_2$  laser drove the excited cluster over the dissociation limit through the absorption of multiple  $\text{CO}_2$  laser photons. They could only access the high frequency N–H stretching motions. They identified two types of N–H oscillators: those associated with the  $\text{NH}_4^+$  core and those of the  $\text{NH}_3$  solvent molecules. For each of these, the frequency of a given transition for a particular subunit (either  $\text{NH}_4^+$  or  $\text{NH}_3$ ) was shifted from that of the free molecule (or ion) by an amount determined by the local environment around the absorbing species. They observed that features of the  $\text{NH}_4^+$  core, assigned to vibrations involved in hydrogen bonds with the solvent  $\text{NH}_3$ 's, were strongly red-shifted from the gas-phase values obtained from velocity modulation

spectroscopy [219–221] due to the strong interactions of the N–H bonds of the ion with the solvent molecules. Vibrational transitions involving the  $\text{NH}_3$  molecules in the first solvation shell ( $n \leq 4$ ) of the complex were significantly less perturbed from their gas phase values because the N–H bond of the ammonias are not themselves involved in the hydrogen bond. The situation was changed for an N–H bond of the first shell ammonia which is involved in a hydrogen bond with a second solvation shell ammonia ( $n \geq 4$ ), although the shift was not as large as that for the ion. The spectral features due to the ion core show some systematic trends with increasing cluster size. The ion core frequencies associated with extensive hydrogen bonding show a gradual blue shift.

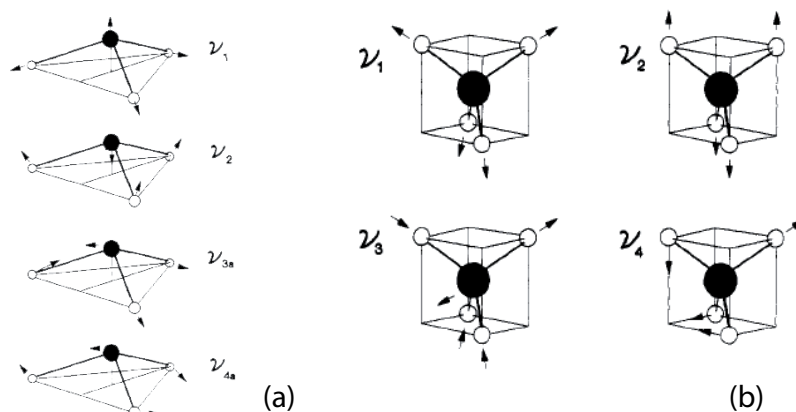


**Figure 6.1:** Normal vibrations of  $\text{NH}_3$  (a) and  $\text{NH}_4^+$  (b). For (a) only one linear combination has been shown for the doubly degenerate modes  $\nu_3$  and  $\nu_4$ . For (b)  $\nu_3$  and  $\nu_4$  are 3-fold degenerate, while  $\nu_1$  and  $\nu_2$  are 1- and 2-fold degenerate, respectively. Arrows in the figure indicate the direction of motion but are not to scale with the amplitude [33].

Ichihashi et al. [222] measured the IR-PD spectra of the  $\text{NH}_4^+(\text{NH}_3)_n$  clusters with  $n=5-8$ , in the  $1045-1091 \text{ cm}^{-1}$  region and carried out Hartree–Fock and Møller–Plesset calculations. They identified the  $\nu_2$  modes of three types of ammonia molecules, namely those directly coordinated to the ammonium ion core but free from other ligands, those directly coordinated to the ammonium ion core and to an ammonia from the second solvation shell, and those from the second solvation shell. Recently, Tono et al. [223] measured the infrared photodissociation spectroscopy of  $\text{NH}_4^+(\text{NH}_3)_n$  cluster ions with  $n=5-8$ , in the  $1000$  to  $1700 \text{ cm}^{-1}$  region. By comparison with DFT calculations they confirmed Ichihashi’s assignment of the ammonia  $\nu_2$  mode to the bands around  $1100 \text{ cm}^{-1}$ , and assigned the ammonium  $\nu_4$  mode to the bands around  $1400 \text{ cm}^{-1}$ .

In the present study the IR-PD spectra of the  $\text{NH}_4^+(\text{NH}_3)_n$  clusters for  $n=1-7$ , are measured in the region from  $600$  to  $1650 \text{ cm}^{-1}$ . The proton is expected to be

symmetrically shared by two  $\text{NH}_3$  molecules in the  $n=1$  cluster and the vibrational frequency of the N–H stretching mode which correspond to the proton transfer is expected to be at  $707\text{ cm}^{-1}$  [224], but this prediction has never been experimentally confirmed. In this study infrared spectra are measured in this region for the first time. With increasing cluster size the evolution of the hydrogen bond network can be studied in a stepwise manner.

## 6.2 Experimental Details

$\text{NH}_4^+(\text{NH}_3)_n$  clusters are produced by electron impact on a supersonic expansion of  $\sim 0.2\%$  ammonia in argon carrier gas (see Section 2.1). The backing pressure is 6 bar for the gas expanding through a  $20\text{ }\mu\text{m}$  orifice. The ZnSe-setup (see Section 2.2) is used to steer FELIX into the tandem mass spectrometer.

For a measurement cycle, the trap is filled for 250 ms and ions are then stored for 150 ms. During all this time FELIX fires two macropulses, producing photofragments if multiple photon dissociation occurs. Immediately after the second macropulse the trap is emptied for 200 ms. Photodissociation manifests itself as a depletion of the parent ion signal and production of charged fragments. The mass selected ion yield of parents and fragments is recorded as a function of FELIX wavelength. This data acquisition cycle is repeated multiple times for every wavelength step, depending on the signal intensity.

To assist the structural assignment quantum chemical calculations were carried out in the group of O. Kühn (Freie Universität Berlin, Germany). For the  $n=2-4$  clusters DFT calculations were used. For the  $n=1$  cluster higher accuracy four dimensional calculations were performed, in which the  $C_{3v}$  symmetry was assumed not to be broken and the length of the six N–H covalent bonds are assumed to be fixed [225, 226].

## 6.3 Results and Discussion

Monitoring the fragment ions has the advantage that the obtained spectrum is background free. On the other hand, fragment ions can also absorb IR radiation and further dissociate, complicating the interpretation of the fragment ion spectra. The two smaller clusters in this study,  $\text{NH}_4^+(\text{NH}_3)_n$  with  $n=1$  and  $n=2$ , show only one fragmentation channel, namely single ammonia loss. For these two clusters, overview spectra with  $0.1\text{ }\mu\text{m}$  step size are at first recorded monitoring both the parent fragmentation and the fragment formation channels. The positions and relative intensities of the bands in the two channels are identical. Then higher resolution spectra with  $0.01\text{ }\mu\text{m}$  step size are recorded only for the fragment formation channel, since they show a better signal to noise ratio. Single ammonia loss is the main dissociation chan-

nel for all clusters studied here. However, larger clusters ( $n \geq 3$ ) also show multiple ammonia loss dissociation channels, with  $n=1$  as the smallest observed fragment. This is due to the fact that (possibly hot) fragment ions absorb IR radiation and further dissociate. Cluster formation enthalpies measured by Searles and Kebarle [214] are  $-27$  kcal/mol for the  $n=0$  to  $n=1$  step and about  $-15$  kcal/mol for other steps up to  $n=4$ . These measured formation enthalpies are consistent with the observation of  $n=1$  as the smallest observed fragment for all  $n \geq 2$  clusters. Therefore, only parent depletion is monitored with higher resolution ( $0.01 \mu\text{m}$  step size) for the larger clusters ( $n \geq 3$ ).

The IR-PD spectra of  $\text{NH}_4^+(\text{NH}_3)_n$  for  $n=1-7$  in the  $600$  to  $1600 \text{ cm}^{-1}$  region are shown in Figure 6.2. The spectra represent the fragment ion formation for the cluster  $n=1$  and 2, and parent ion depletion for  $n \geq 3$ , in dependence of the FELIX wavelength. The plots for the clusters  $n=1$  and 2 are mirrored on the horizontal axis for better comparison with all other spectra. The data are normalized with respect to the most intense peak.

The most intense peak in all spectra shifts monotonically from  $1327 \text{ cm}^{-1}$  for  $n=1$  to  $1120 \text{ cm}^{-1}$  for  $n=7$ . In the portion of the spectra with energies lower than the most intense peak, strong bands can be detected only for the  $n=1$  and 4 clusters. Structures with similar intensities are found in all spectra at energies higher than  $1400 \text{ cm}^{-1}$ . According to the known vibrational frequencies reported in Table 6.1, the  $\nu_2$  and  $\nu_4$  modes of both bare ammonia and bare ammonium are active in the spectral region covered by this study.

	$\text{NH}_4^+$ ( $T_d$ Symmetry)		$\text{NH}_3$ ( $C_{3v}$ Symmetry)
$\nu_1$ :	$3270 \pm 25$ [227]	$\nu_1$ :	$3336.21$ [228]
$\nu_2$ :	$1669$ [229]	$\nu_2$ :	$950$ [230]
$\nu_3$ :	$3343.28$ [221]	$\nu_3$ :	$3444$ [230]
$\nu_4$ :	$1447.22$ [219]	$\nu_4$ :	$1627$ [230]

**Table 6.1:** Vibration frequencies for  $\text{NH}_4^+$  and  $\text{NH}_3$  (in  $\text{cm}^{-1}$ ).

### 6.3.1 Protonated Ammonia Dimer

Hydrogen bonding in the protonated ammonia dimer is considerably stronger than in all larger clusters of this study. This leads to an equal sharing of the central proton by the two ammonia units, similar to the protonated water dimer [231]. The most intense band in the  $n=1$  spectrum is found at  $1327 \text{ cm}^{-1}$  (see Figure 6.3). In the portion of the spectrum at lower energies three main bands are measured at  $742$ ,  $938$ , and  $1101 \text{ cm}^{-1}$  (see also Table 6.2), while in the higher energy region

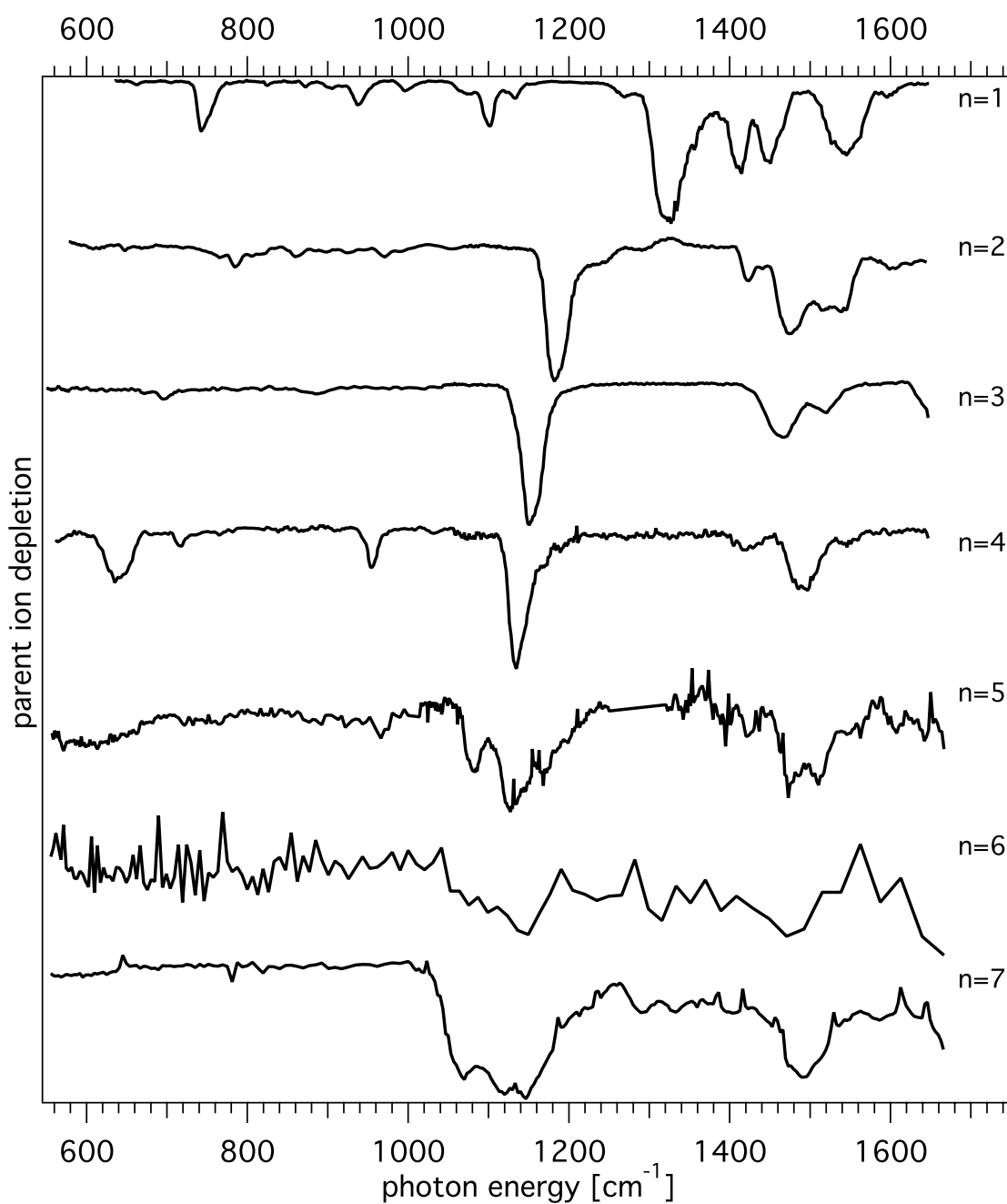


**Figure 6.2:** The IR-PD spectra of  $\text{NH}_4^+(\text{NH}_3)_n$  for  $n=1-7$ . Fragment ion formation in dependence of the FELIX wavelength is monitored for  $n=1$  and 2. For the cluster  $n \geq 3$  parent ion depletion is monitored.

two intense bands with similar width and intensity appear at 1415 and 1451  $\text{cm}^{-1}$ , and a broader feature appears at 1545  $\text{cm}^{-1}$ . Calculations find the fundamental of

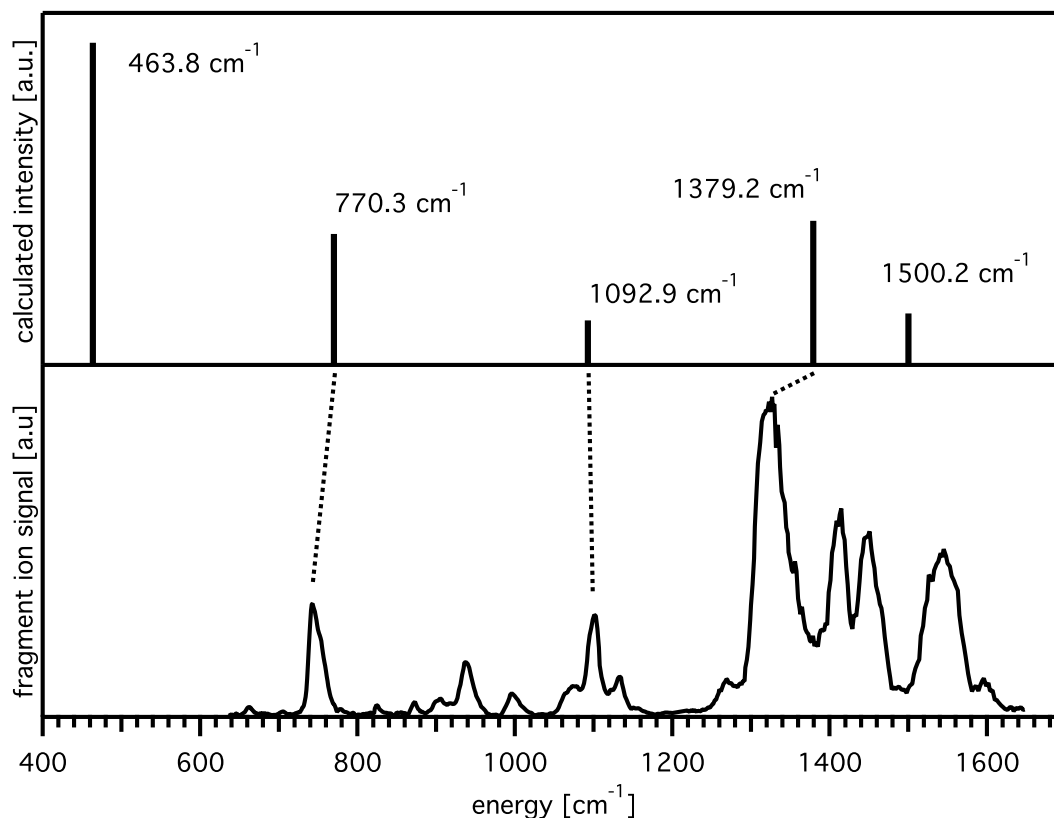


**Figure 6.3:** IR-PD spectrum of the protonated ammonia dimer (bottom), measured by monitoring the  $\text{NH}_4^+$  fragment ion yield, and calculations from the 4D model (top).

hydrogen transfer at 464  $\text{cm}^{-1}$ , outside the measured region. Three calculated modes are assigned to bands observed in the IR-PD spectrum. The mode calculated at 1379  $\text{cm}^{-1}$  is due to the anti-symmetric umbrella like angular motion, which agrees with the measured band at 1327  $\text{cm}^{-1}$ . The combination of the proton transfer and the  $\text{NH}_3\text{--NH}_3$  stretching modes is calculated at 770  $\text{cm}^{-1}$  and is assigned to the band observed at 742  $\text{cm}^{-1}$  in the experiments. Another vibrational mode is due to the 1 + 2 combination of these modes and is assigned to the band measured at 1101  $\text{cm}^{-1}$ . A mode due to the bend of an ammonia unit is calculated at 1500  $\text{cm}^{-1}$ . However, the spectral region between 1300 and 1600  $\text{cm}^{-1}$  is expected to be dominated by the antisymmetric stretches of the  $\text{NH}_3$  and  $\text{NH}_4^+$  units, although they may well be significantly shifted by the strong hydrogen bond. These modes cannot be studied

under the present theoretical approximation since the coordinates involved in their vibrations are frozen in computations. Indeed it is clear that the theoretical model used here is not sufficient to account for all observed bands, but it gives a reasonable agreement for the two modes in which the proton transfer is involved, measured at 742 and 1101  $\text{cm}^{-1}$ . In the lower region of the spectrum other bands of smaller intensities are observed and are tentatively assigned to overtones and combination bands, due to the high power required to achieve photodissociation.

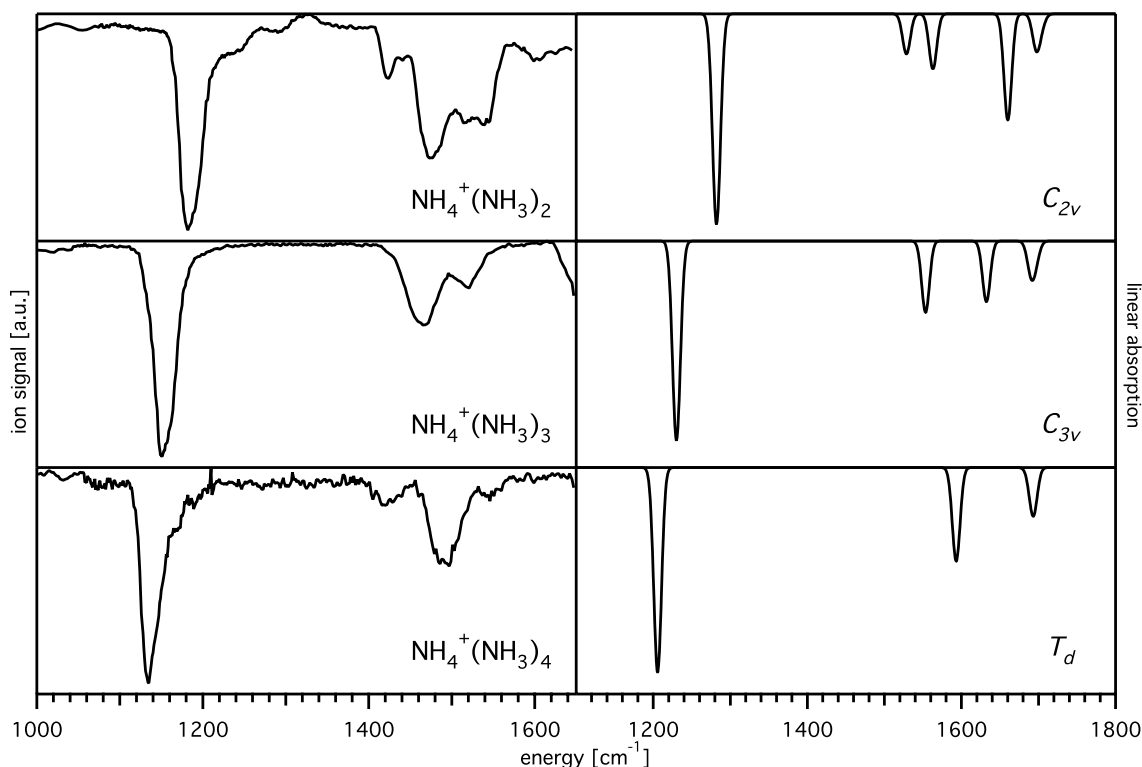


**Figure 6.4:** IR-PD spectra for  $\text{NH}_4^+(\text{NH}_3)_n$  with  $n=2-4$  (left) and linear IR absorption from DFT calculations (right).

### 6.3.2 Protonated Ammonia Trimer, Tetramer, and Pentamer

The IR-PD spectra of  $\text{NH}_4^+(\text{NH}_3)_n$  for  $n=2-4$  in the 1000 to 1650  $\text{cm}^{-1}$  region are shown in Figure 6.4 together with DFT calculations, between 1100 and 1800  $\text{cm}^{-1}$ . The calculated frequencies are systematically too high and can be corrected by introducing a scaling factor. DFT calculations find minimum energy structures for the clusters with  $n=2-4$  with  $C_{2v}$ ,  $C_{3v}$ , and  $T_d$  symmetry, respectively; where every ammonia molecules is hydrogen bonded to the ammonium ion core. These results are consistent with previous studies [217, 218, 222]. The 1000–1650  $\text{cm}^{-1}$  region is



dominated by an intense band between 1100 and 1200  $\text{cm}^{-1}$ . This band shifts from 1182  $\text{cm}^{-1}$  for the  $n=2$  cluster, to 1151  $\text{cm}^{-1}$  for  $n=3$ , to 1135  $\text{cm}^{-1}$  for  $n=4$ . DFT calculations (not scaled) reproduce this monotone red shift with 1281, 1230, and 1205  $\text{cm}^{-1}$  for  $n=2, 3$ , and 4, respectively. Consequently, these modes are assigned to the ammonia umbrella vibration ( $\nu_2$ ), strongly perturbed by the ammonium ion. The perturbation induced by the ammonium ion decreases with increasing number of ammonia molecules and the band moves towards the frequency of the unperturbed  $\nu_2$  mode measured at 950  $\text{cm}^{-1}$  in bare gas phase ammonia [230]. The weakening of the interaction between the ammonium ion and ammonia molecule with increasing  $n$  is reflected in the N–N distance between the central ammonium core and each ammonia molecule in the optimized structures: 2.833, 2.862, and 2.929 Å, for  $n=2, 3$ , and 4, respectively. It appears, that the position of this  $\nu_2$  ammonia peak is very sensitive to the bond strength between ammonia and the ammonium ion. It is therefore interesting to note that neither splitting nor broadening of this peak for the clusters with  $n=1-4$  is observed. Thus, all ammonium-ammonia bonds must be equivalent within every cluster.

Between 1400 and 1600  $\text{cm}^{-1}$ , three main bands for  $n=2$ , two bands for  $n=3$ , and one main band with smaller structures at the two sides for  $n=4$  are observed. In this region the ammonium antisymmetric stretch  $\nu_4$  is expected to be active [219], and the number of bands is consistent with the calculated symmetries. The three fold degenerate  $\nu_4$  mode of  $T_d$  symmetry in the  $n=4$  cluster splits into two and three bands in the  $n=3$  and  $n=2$  clusters, respectively. Schwarz [217] measured the first overtone of this mode for the  $n=4$  cluster at 3087  $\text{cm}^{-1}$ , whereas Lee and coworkers [218] measured it at 3095  $\text{cm}^{-1}$ . These values were consistent with the present observation of a small band at 1546  $\text{cm}^{-1}$ , assuming negligible anharmonicity. However, the most intense band in the region is found at 1497  $\text{cm}^{-1}$ , which would imply a negative anharmonicity if assigned to the  $\nu_4$  vibration. DFT calculations find the ammonium  $\nu_4$  mode at 1593  $\text{cm}^{-1}$ , and the ammonia  $\nu_4$  mode at 1689  $\text{cm}^{-1}$ . For the  $n=3$  cluster, maxima for the two bands are found at 1468 and 1521  $\text{cm}^{-1}$  ( $\Delta E=53 \text{ cm}^{-1}$ ), while calculations return the split  $\nu_4$  ammonium mode at 1554 and 1632  $\text{cm}^{-1}$  ( $\Delta E=78 \text{ cm}^{-1}$ ). For the  $n=2$  cluster, maxima in the IR-PD spectrum are found at 1424, 1475, and 1540  $\text{cm}^{-1}$  (although this last band is broader and seems to consist also of a second peaks with maximum at 1518  $\text{cm}^{-1}$ ), with relative distances between maxima of 51 and 65  $\text{cm}^{-1}$ . Calculations find the three energies of the  $\nu_4$  mode at 1529, 1563, and 1660  $\text{cm}^{-1}$ , with splittings of 34 and 97  $\text{cm}^{-1}$ . The blue shift with increasing  $n$  of the ammonium  $\nu_4$  mode is consistent with the blue shift observed by Schwarz [217] for the  $\nu_4$  mode between  $n=3$  and 4. Calculations indicate the presence of the  $\nu_4$  ammonia mode about 1690  $\text{cm}^{-1}$ , roughly at the same energy for all three clusters. Yet, IR-PD spectra do not present any band at an energy higher than the bands assigned to the ammonium  $\nu_4$  at a fixed position in all three clusters; only the  $n=2$  cluster has a weak band at 1600  $\text{cm}^{-1}$ . Thus, either the ammonia  $\nu_4$  mode is shifted outside the measured region,

or is included in the ammonium bands (and this would explain the extra peak in the  $n=2$  cluster and one side band in the  $n=4$  cluster), or its position does not appear at the same energy in the three spectra. However, this calculated mode cannot be assigned to any feature recorded in the IR-PD spectra.

At longer wavelengths the spectrum presents some remarkable aspects. Evidence for the proton transfer is only expected for the case  $n=1$ , but we find three clear absorption bands also for  $n=4$ . No fundamentals are predicted in the region between 600 and 1100  $\text{cm}^{-1}$  by DFT calculations and therefore one can only speculate on their origin. Here, two possible assignments are suggested. (i) DFT calculations for the  $n=4$  cluster predict a strong absorption around 400  $\text{cm}^{-1}$ , corresponding to frustrated rotation of the  $\text{NH}_3$  molecules. Therefore, the bands between 600 and 1100  $\text{cm}^{-1}$  can be assigned to combination bands involving this intense vibrational mode. (ii) The two major bands in this region for the  $n=1$  cluster are assigned to combinations of the  $\text{NH}_3-\text{NH}_3$  stretching mode with the proton transfer mode, on the basis of higher level calculations carried out for this species. Since the N-N distance increases with increasing cluster size, as discussed above, the fundamental  $\text{NH}_3-\text{NH}_3$  stretching mode must also progressively shift to lower energies. Therefore, the two bands observed for the  $n=4$  cluster at 635 and 955  $\text{cm}^{-1}$  can be assigned to analogous combinations as in the  $n=1$  case, indicating the presence of a shared proton.

### 6.3.3 Larger Clusters

The spectrum for  $n=6$  has very low resolution and carries little information. In the  $n=5$  and 7 clusters (see Figure 6.2), the band assigned to the  $\nu_2$  ammonia mode stays at about 1120  $\text{cm}^{-1}$  while a new band appears at each side. The experimental values of 1083.5, 1127, and 1168  $\text{cm}^{-1}$  for  $n=5$  are assigned to the  $\nu_2$  mode of three different kinds of ammonia molecule. The ammonia from the second solvation shell is active at 1083.5  $\text{cm}^{-1}$ . This ammonia is bound to another ammonia molecule from the first shell, whose  $\nu_2$  mode is found at 1168  $\text{cm}^{-1}$ . The remaining three ammonia molecules in the first shell are found at 1127  $\text{cm}^{-1}$ , similarly to the  $n=4$  case. In the  $n=7$  cluster, only minor changes in the frequencies are observed but the intensities of the bands due to the ammonia molecules in the second shell increase significantly as it can be expected. These findings are consistent with the results by Ichihashi et al. [222] and Tono et al. [223].

Interestingly, the spectrum for  $n=5$  measured by Tono et al. [223] appears much better resolved than in the present study for the bands around 1100  $\text{cm}^{-1}$  but poorer resolved for the bands above 1400  $\text{cm}^{-1}$ . In particular, in the present study two clear bands appear at 1473 and 1510.5  $\text{cm}^{-1}$  and three minor features at 1395, 1608, and 1642  $\text{cm}^{-1}$ , where Tono's spectrum shows only a maximum at 1490  $\text{cm}^{-1}$  with a shoulder about 1520  $\text{cm}^{-1}$  and a small peak at 1405  $\text{cm}^{-1}$ . Reasons for the observed differences can be found in different optics used, for example, which would yield differ-

Cluster	Position of observed bands ( $\text{cm}^{-1}$ )
$\text{NH}_4^+(\text{NH}_3)$	1596, 1545, 1526(s), 1451, 1415, 1356(s), 1327, 1269, 1133, 1101, 1075, 996, 938, 905, 873, 824, 742, 661
$\text{NH}_4^+(\text{NH}_3)_2$	1600, 1540, 1518, 1475, 1424, 1290, 1244(s), 1182, 971, 862, 805, 784, 765, 648
$\text{NH}_4^+(\text{NH}_3)_3$	1521, 1468, 1151, 888, 695, 672
$\text{NH}_4^+(\text{NH}_3)_4$	1546, 1497, 1422, 1497, 1170(s), 1135, 1032, 955, 719, 635
$\text{NH}_4^+(\text{NH}_3)_5$	1642, 1608, 1510.5, 1473, 1422.5, 1395, 1168, 1127, 1083.5, 961.5, 893, 877, 766, 722
$\text{NH}_4^+(\text{NH}_3)_6$	1471, 1316, 1150
$\text{NH}_4^+(\text{NH}_3)_7$	1493, 1403, 1330, 1289, 1143, 1120, 1070, 781

**Table 6.2:** Experimental vibrational frequencies (in  $\text{cm}^{-1}$ ) of the protonated ammonia clusters,  $\text{NH}_4^+(\text{NH}_3)_n$ , in the 600–1650  $\text{cm}^{-1}$  range, determined from the respective IR-PD spectra, measured monitoring fragment ions mass-selectively for  $n=1$  and 2, and monitoring parent ion depletion for  $n \geq 3$ . Vibrational frequencies are determined from band maxima or estimated based on observable shoulders (s) formed by overlapping transitions.

ent laser powers in different wavelength regions, or different FEL performances. The agreement of the measured spectrum from the present work and DFT calculations by Tono et al. is satisfactory, yielding the following assignments: the bands at 1473 and 1510.5  $\text{cm}^{-1}$  are assigned to the  $\nu_4$  mode of the ammonium ion and the two bands above 1600  $\text{cm}^{-1}$  are assigned to modes involving the  $\nu_4$  mode of the ammonias. The band at 1395  $\text{cm}^{-1}$  (1405  $\text{cm}^{-1}$  in the work by Tono) remains unassigned.

## 6.4 Summary

The protonated ammonia clusters,  $\text{NH}_4^+(\text{NH}_3)_n$  with  $n=1-7$ , were studied by IR-PD spectroscopy in the 600–1700  $\text{cm}^{-1}$  region. Data recorded in the lower energy region are of particular interest, because they directly probe the modes in which proton transfer is involved. For the  $n=1$  cluster two absorption bands are assigned to modes in which combination of the proton transfer with  $\text{NH}_3-\text{NH}_3$  stretch is involved, measured at 742 and 1101  $\text{cm}^{-1}$ . This confirms 4D calculations that predict the fundamental frequency of proton transfer at 464  $\text{cm}^{-1}$ , against previous calculations that found the frequency of proton transfer at 707  $\text{cm}^{-1}$  [224]. For  $n=1-4$  clusters a monotone shift of the ammonia umbrella mode ( $\nu_2$ ) with increasing cluster size is observed and the absorption band is not split. This indicates a decreasing bond strength between

$\text{NH}_3$  and  $\text{NH}_4^+$  species with increasing cluster size and that all ammonia molecules are equivalent within each cluster. Surprisingly, evidence for proton transfer is also found in the  $n=4$  cluster, contrary to any expectation.

For the larger clusters, the here presented results agree with previous studies by Tono [223] and Ichihashi [222]. It is found that the  $\nu_2$  band of  $\text{NH}_3$  splits into three according to the coordination sites in the cluster ions; three observed peaks at about 1083, 1127, and 1168  $\text{cm}^{-1}$  can be assigned to  $\text{NH}_3$  in the second solvation shell,  $\text{NH}_3$  in the first solvation shell, which is not bound to other ammonia molecules, and  $\text{NH}_3$  in the first solvation shell, which is bound to  $\text{NH}_3$  in the second solvation shell. This clearly confirms the shell closure with 4 ammonia molecules.